A direct method for the extension of FastSim under non-Hertzian contact conditions

J. Gómez-Bosch, J. Giner-Navarro, J. Carballeira & L. Baeza

Published online: 17 Sep 2022.

Submit your article to this journal

View related articles

View Crossmark data

IA*VSD*

Taylor & Francis
Taylor & Francis Group

Check for updates

A direct method for the extension of FastSim under non-Hertzian contact conditions

J. Gómez-Bosch, J. Giner-Navarro, J. Carballeira and L. Baeza

I2MB, Universitat Politècnica de València, Valencia, Spain

ABSTRACT

In wheel-rail contact mechanics, there coexist different models characterised by their ability to reproduce the real phenomenon and the time associated with computing the solution. In simulation of the vehicle dynamics, the increase in the computational performance places researchers close to a horizon in which it is possible to implement the most realistic theories (Variational Theory or finite elements), although at present the use of these models is mainly limited to offline calculations, far from real-time simulation. In this context, this work presents a tangential contact theory that is an intermediate point between simplified models (unable to model non-Hertzian contact) and more realistic models (whose complexity triggers simulation times). The tangential contact model proposed is based on the FastSim algorithm, whose precision comes from the algorithm convergence to the results of an exact adhesion theory (i.e. when creepages tend to zero). The impossibility of considering Kalker's Linear Theory as an adjustment method when the hypotheses of the Hertzian model are not fulfilled leads to the adoption of the Kalker's steady-state CONTACT version in adhesion conditions. The calculations presented through the proposed algorithm provide errors for creep forces lower than 4% with computational times one order lower than the Variational Theory.

1. Introduction

The calculation cost associated with the simulation of the railway vehicle dynamics is well-known to be highly conditioned by the formulation of the wheel-rail contact problem. Although some authors have opted to use pre-calculated tables of creep forces and moments as an approach to deal with this problem as alternative for vehicle dynamics simulation [1], this difficulty has usually been solved by the implementation of simplified contact theories. These models achieve acceptable results and low computational costs through less-realistic assumptions of the contact problem, such as Vermeulen and Johnson [2], Shen et al. [3] or Polach's [4] model. Among those simplified theories, one of the most widespread method is FastSim [5] due to its accuracy and low computing times. The

---

Supplemental data for this article can be accessed here. https://doi.org/10.1080/00423114.2022.2120022

FastSim algorithm is based on the full-adhesion solution and assumes that the surface displacements at a point on the contact area are only dependent on the contact tractions at that same point through the so-called flexibility parameters. These parameters are obtained by matching the force results of the simplified full-adhesion solution with those of an exact theory, which also assumes adhesion over the entire contact area. In the original FastSim algorithm, this exact theory is Kalker's Linear Theory [6] and the flexibility parameters are calculated by means of a closed-form expression of Kalker's creepage coefficients that linearly relate the longitudinal, tangential creep forces with the creepages. However, despite its advantages, FastSim presents certain limitations that have led different authors to modify the model to extend its applicability to non-elliptical contact areas. Despite the full-adhesion solution does not assume the Hertzian hypothesis, the Linear Theory does so, thus, the original FastSim algorithm is limited to elliptical contact areas, namely Hertzian contact conditions.

In order to extend FastSim applicability to non-Hertzian conditions, it is needed to obtain the flexibility parameters for non-elliptical contact areas. To that aim, several authors have proposed different FastSim extensions to non-Hertzian conditions that can be distinguished depending on how the flexibility parameters are computed: (a) equivalent ellipse methods [7–11], in which the contact area is associated with one or more equivalent ellipses, obtaining the flexibility parameters from these equivalent ellipses geometry (as it is done in the original FastSim algorithm); and (b) direct methods [12, 13], in which a different theory to Kalker's Linear Theory is used to compute the flexibility parameters for arbitrary contact areas.

The equivalent-ellipse methods are computationally much more efficient since solving each specific case is not needed. This improvement in computational cost has a loss of accuracy as counterpart since flexibility parameters are not directly computed from the original geometry. Different alternatives have been proposed regarding the number of ellipses that make up the contact area and how its dimensions are obtained. Piotrowski and Kik [7] divided the contact patch into one or more separate regions to which an equivalent ellipse is related to each one. The semi-axes of this equivalent ellipse are obtained from the geometry of the original contact, ensuring that: (a) both traces have the same area; (b) the ratio of the axes for the equivalent ellipse is equal to the ratio of the sides of the rectangle that circumscribes the original contact area. This method achieves an error of 9% for tangential forces when only spin creepage is acting [14]. A later paper extended the study through the comparison with several methods, showing that Piotrowski and Kik's model presented greater errors about 10 or even 15% [15]. Alonso and Giménez [8] proposed to associate the contact area with two equivalent semi-ellipses (whose semi-axes were obtained from the geometry of the original contact area) by assuming that the total area and the second area moments of inertia are the same in the non-Hertzian and the equivalent Hertzian areas. Results with errors generally lower than 10% compared with Kalker's Variational Theory [16] were obtained for different combinations of creepages, according to results presented in Ref. [8]. Piotrowski et al. [9] focused on a particular case of contact area based on their previous work [7]: when the wheel crosses a corrugated rail, a characteristic contact shape appears, which can be approximated to two semi-ellipses; the resulting area shows the advantage of having quasi-Hertzian characteristics and being regularisable based on two geometric parameters (just like ellipses). Taking these characteristics into

account, the authors proposed to build a look-up table for non-Hertzian contact (similar to the one proposed by Kalker in Ref. [1]) in order to speed up the calculations of the tangential contact forces for non-Hertzian areas. For different cases analysed in this work, maximum errors of 9.4% are achieved with respect to Kalker's Variational Theory [13].

Linder [10] and Ayasse and Chollet [11] proposed to divide the contact patch into strips parallel to the longitudinal direction with a virtual ellipse associated with each of them; therefore, the flexibility parameters were calculated for the ellipse corresponding to each strip. The way in which these ellipses are obtained is different in each work. Linder maintained the lateral dimensions of each ellipse identical to the size of the original contact area and, with that dimension fixed, the longitudinal one is chosen, thus the strip fits within the resulting equivalent ellipse. Instead, Ayasse and Chollet calculated these ellipses based on the relative curvatures in the centre of the strip. According to the studies carried out by Sichani et al. [14], the errors for the tangential force in the case of steady-state pure spin are about 14% for the method in Ref. [10] and 108% in [11]. Unlike the rest of the methods presented in which the entire contact area has the same contact angle, in Ref. [11] each strip has a different contact angle and, hence, a different value for spin, thus explaining this disproportionate error. Notwithstanding this particular study, calculations carried out in Ref. [15] show errors between 10 and 15% under different scenarios for the method presented by Ayasse and Chollet [11].

Regarding direct methods, Kalker proposed a modification for his original algorithm [13] based on determining the flexibility parameters by means of minimising the difference between the displacements calculated through the simplified theory and those produced by a certain tangential traction distribution (usually, the traction distribution under full-slip conditions) calculated through Cerruti's equations. According to the results shown in Ref. [8], this method leads to a significant loss of accuracy even for Hertzian contact cases, with errors reaching approximately 15% for the flexibility parameters.

In the same line of direct methods, Knothe and Hung [12] contributed with an alternative method by means of the computation of the flexibility parameters for each specific patch by equating the forces of the full-adhesion solution with those obtained after solving the tangential exact contact problem [13] for non-elliptical contact areas assuming full adhesion. To solve the corresponding equations, the contact area is discretised into strips parallel to the rolling (or longitudinal) direction, and the contact traction distributions in the longitudinal and lateral directions are approximated to quadratic polynomials in the longitudinal direction. This polynomial approximation is implemented in this work, giving deviations about 4% for the creepage coefficients compared with the ones obtained through Kalker's Linear Theory.

In the present paper, a methodology for the calculation of the tangential forces and tractions over the wheel-rail contact area for non-Hertzian contact conditions is proposed based on the FastSim algorithm. This new proposal for the FastSim generalisation, which will be called nH-FastSim along the paper, can be included within the direct methods since the flexibility parameters are computed through an alternative exact method. Instead of using the Linear Theory for calculating the flexibility parameters, this paper proposes the use of the steady-state CONTACT version [13] assuming infinite friction coefficient. The CONTACT method developed by Kalker allows solving the unsteady and the steady-state tangential contact problem for non-Hertzian areas. The methodology for the calculation of the flexibility parameters is deduced by forcing that the extension of FastSim provides

the same results as the steady-state CONTACT version when it is assumed that the entire contact area is in adhesion (i.e. infinite friction coefficient).

The structure of this paper is as follows. Section 2 presents the nH-FastSim algorithm proposed. The formulation of the method depending on the flexibility parameters is detailed in subsection 2.1. The calculation of the flexibility parameters is presented in the following two subsections: subsection 2.2 reproduces for clarity and completeness the Kalker's steady-state CONTACT version when infinite friction coefficient is assumed (adhesion model); subsection 2.3 imposes that the contact forces provided by CONTACT and nH-FastSim coincide to obtain the flexibility parameters. Section 3 evaluates the steady-state CONTACT version for adhesion areas through the calculation of the creepage coefficients. Section 4 shows results of nH-FastSim that can contribute to the validation of the method as a simulation tool in railway dynamics. Finally, Section 5 presents the most relevant conclusions of this paper.

In the present document, the results from CONTACT refers to a version of the program that was developed by the authors, and it does not correspond neither to the original software developed by Kalker nor any other commercial package.

2. Non-Hertzian FastSim extension development

2.1. Fastsim extension algorithm

In order to model the contact problem between the wheel and the rail, a moving reference system $\mathbf{X}_1\mathbf{X}_2\mathbf{X}_3$ is adopted, whose origin is the centre of pressure associated with the normal traction distribution. The $\mathbf{X}_1$-axis corresponds to the rolling direction, the $\mathbf{X}_3$-axis is normal to the contact area (being the positive direction towards the wheel), and the $\mathbf{X}_2$-axis is associated with the lateral direction, positive according to a right-handed frame of reference, as depicted in Figure 1.
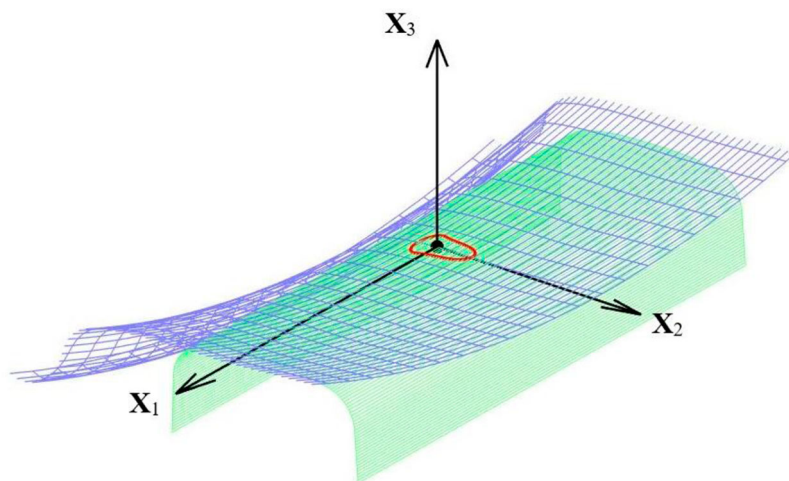

Figure 1. Frame of reference $\mathbf{X}_1\mathbf{X}_2\mathbf{X}_3$ centred at the centre of pressure between the rail (lower body) and the wheel (upper one). The small closed curve sketches the contact patch.

Unlike the discretisation of the contact area proposed in the original FastSim algorithm, particularly adapted to an elliptical patch, a regular mesh of rectangles is now adopted to address a general contact area as used in CONTACT, in which the potential contact area is meshed. Tractions are assumed to be constant in each element of the mesh in contact. For the e-th element, the coordinates of its centre are defined as (x_1^e, x_2^e), corresponding to a point of the contact plane $\mathbf{X}_1 \mathbf{X}_2$.

Non-conformal contact conditions are adopted. Assuming elastic quasi-identity hypotheses for the solids in contact [13], the solution of the normal contact problem provides the value of the normal traction in each element of the contact area independently of the tangential contact problem. Its value in the e-th element can be obtained through any exact (e.g. normal CONTACT) or simplified method (see Refs. [7, 11]). Following the same procedure than in the original FastSim algorithm, it is proposed to modify the normal traction distribution used to discern whether an element is under slip or adhesion conditions. To do so, the original normal traction distributions along strips in the x_1-direction are approximated to parabolas to extend the method to a non-elliptical patch [5]. The criterion followed to get these parabolas is that the modified distribution maintains the size of the contact area and the level of the normal contact force F_3. Following this criterion, equations for the parabolas can be obtained:

$$p_3^e = h^e \left(1 - 4 \left(\frac{x_1^e - x_c^e}{x_\ell^e - x_t^e} \right)^2 \right), \tag{1}$$

where p_3^e is the modified normal traction of the e-th element, h^e is the height of the parabola (obtained by equalling the normal contact force on each strip with both distributions), x_ℓ^e and x_t^e are the coordinates of the leading and trailing edge of the contact area and x_c^e is the midpoint between the leading and trailing edges of the contact area; parameters h^e, x_ℓ^e, x_t^e and x_c^e depend on the lateral coordinate of the current element x_2^e.

By approximating the normal tractions to parabolas, results are considerably more accurate through FastSim since an elliptic reference traction distribution prevents slip at the leading edge of the contact area [17]. In the same reference, it is also demonstrated that a parabolic traction distribution reproduces better the subdivision of the contact area into adhesion and slip regions.

From this point on, the methodology follows the original FastSim algorithm, so that the tractions for the e-th element of the mesh under adhesion conditions $\bar{p}_\tau^e$ along to the τ direction ($\tau = 1, 2$) are calculated as

$$\bar{p}_1^e = \left(\frac{\xi}{L_1} - \frac{\phi}{L_3} x_2^e \right) (x_1^e - x_\ell^e), \tag{2}$$

$$\bar{p}_2^e = \left(\frac{\eta}{L_2} + \frac{1}{2} \frac{\phi}{L_3} (x_1^e + x_\ell^e) \right) (x_1^e - x_\ell^e), \tag{3}$$

where ξ, η and ϕ are the longitudinal, lateral and spin creepages, respectively; and L_1, L_2 and L_3 are the flexibility parameters.

Equations (2) and (3) can be written also in matrix form as

$$\bar{\mathbf{p}} = \mathbf{B} \, \mathbf{L}^{-1} \, \boldsymbol{\xi}, \tag{4}$$

being $\bar{\mathbf{p}}$ the vector that contains tangential tractions in the elements of the mesh under full-adhesion hypothesis, $\boldsymbol{\xi} = \{\xi, \eta, \phi\}^T$ the creepage vector, $\mathbf{B}$ is a matrix with the geometrical terms in Equations (2) and (3), and $\mathbf{L}$ is the following diagonal matrix

$$\mathbf{L} = \begin{bmatrix} L_1 & 0 & 0 \\ 0 & L_2 & 0 \\ 0 & 0 & L_3 \end{bmatrix}. \tag{5}$$

In order to maintain a coherent formulation with the formulation presented in the paper, the vector of tangential tractions $\bar{\mathbf{p}}$ is ordered according to the following scheme

$$\bar{\mathbf{p}} = \begin{bmatrix} \bar{p}_1^1 & \bar{p}_2^1 & \bar{p}_1^2 & \bar{p}_2^2 & \cdots & \bar{p}_1^{N_C} & \bar{p}_2^{N_C} \end{bmatrix}^T, \tag{6}$$

being N_C the number of elements in contact.

Tractions obtained through Equations (2) and (3) in each element must be corrected to consider the possible slip of the element. To do so, each element must be checked to verify if the adhesion condition is met

$$||(\bar{p}_1^e, \bar{p}_2^e)|| \leq \mu p_3^e, \tag{7}$$

where $||.||$ denotes the vector norm and μ is the friction coefficient. If the condition in Equation (7) is fulfilled, the stick solution for the element is valid, that is, $p_\tau^e = \bar{p}_\tau^e$. If the condition is not met, the traction in the element is formulated as

$$p_\tau^e = \frac{\mu p_3^e}{||(\bar{p}_1^e, \bar{p}_2^e)||} \bar{p}_\tau^e, \quad \tau = 1, 2. \tag{8}$$

In the original FastSim algorithm, these flexibility parameters are obtained through the creepage coefficients C_{ij} [13], the ellipse semiaxes of the contact area, a and b, and the shear modulus G, as follows

$$L_1 = \frac{8a}{3C_{11}G}, \quad L_2 = \frac{8a}{3C_{22}G}, \quad L_3 = \frac{\pi a^{3/2}}{4\sqrt{b}C_{23}G}. \tag{9}$$

These creepage coefficients C_{ij}, also known as Kalker coefficients, are used for tangential forces calculation in Kalker's Linear Theory. They are obtained by the numerical resolution of elliptic integrals, using a suitable series expansion truncated after a small number of terms, being a good approximation to the real values. As it is explained in [13], these parameters are function of the ellipse geometry via its semiaxes ratio a/b and the material properties through the Poisson's ratio υ.

At this point, it is come up with a methodology to calculate the flexibility parameters L_1, L_2 and L_3 for non-elliptical areas. For this, it is needed to have a numerical methodology to solve the full-adhesion steady-state tangential contact problem for non-elliptical areas. This numerical methodology is Kalker's CONTACT when an infinite friction coefficient is assumed, and its formulation is reproduced for completeness in subsection 2.2. The procedure through which the flexibility parameters are obtained is presented in subsection 2.3.

2.2. *Kalker's CONTACT for adhesion areas*

The CONTACT algorithm [13] provides the solution of the tangential contact problem assuming non-Hertzian contact conditions. The steady-state CONTACT version will be adopted in the present section with the purpose of developing the formulation for adhesion conditions (infinite friction coefficient).

According to the steady-state CONTACT, the tangential problem is solved based on the equation that combines kinematics in contact with the constitutive relationships associated with an infinite half-space, which is

$$\mathbf{s} = \mathbf{w} - \frac{V}{\Delta x_1}(\mathbf{A} - \mathbf{A}^0)\,\mathbf{p}, \tag{10}$$

where $\mathbf{s}$ is the vector that contains the local slip velocities of the collocation points, V is the speed (or rolling velocity) of the wheel, Δx_1 is the traversed distance of the wheel associated with finite differences (Δx_1 should be taken as the size of the element on the longitudinal direction [13]), $\mathbf{p}$ is the vector with the steady-state tangential tractions in the elements of the mesh, $\mathbf{A}$ is the matrix of the elastic influence coefficients that relate the displacements at the collocation points and the tangential tractions in the elements, $\mathbf{A}^0$ associates the displacements at the collocation points with the traction distribution applied on the mesh at the previous wheel position displaced Δx_1 backwards, and $\mathbf{w}$ is the vector with the velocities of the wheel associated with the undeformed configuration. The vector $\mathbf{w}$ is computed according to the linear relationship

$$\mathbf{w} = V\mathbf{D}^{\mathrm{T}}\,\boldsymbol{\xi}\,, \tag{11}$$

being $\mathbf{D}$ the matrix that contains the coordinates of the collocation points associated with the elements, which can be formulated as

$$\mathbf{D} = \begin{bmatrix} 1 & 0 & 1 & 0 & \cdots & 1 & 0 \\ 0 & 1 & 0 & 1 & \cdots & 0 & 1 \\ -x_2^1 & x_1^1 & -x_2^2 & x_1^2 & \cdots & -x_2^{N_C} & x_1^{N_C} \end{bmatrix}, \tag{12}$$

where x_τ^e is the coordinate of the e-th element along the $\mathbf{X}_\tau$-direction, with $\tau = 1, 2$. Matrix $\mathbf{D}$ is also used to calculate the resultant forces $\mathbf{F}$ as

$$\mathbf{F} = S\,\mathbf{D}\,\mathbf{p}, \tag{13}$$

being $\mathbf{F} = \{F_1, F_2, M_3\}^{\mathrm{T}}$ a vector that contains the contact forces and spin moment, and S the area of the mesh element.

With the purpose of computing the flexibility parameters, it is assumed full-adhesion hypothesis. To do so, zero-slip velocity is imposed in Equation (14):

$$\bar{\mathbf{p}} = \frac{\Delta x_1}{V}(\mathbf{A} - \mathbf{A}^0)^{-1}\,\mathbf{w}. \tag{14}$$

The above equation is a numerical model for non-Hertzian contact areas that is analogous to Kalker's Linear Theory. Equation (14) is linear and its computation is much faster than CONTACT based on Kalker's TANG algorithm and Newton iteration for the subsequent nonlinear systems when finite friction coefficient is assumed. From the tangential

tractions under adhesion conditions obtained, the flexibility parameters can be computed as detailed in the next subsection.

Besides for computing flexibility parameters, this steady-state CONTACT is also used as a reference solution. In that case, the solution of Equation (10) is obtained by means of regularisation of the Coulomb's law, through the methodology that is explained in the Appendix of the present paper.

2.3. Flexibility parameters calculation

As done in the original algorithm, the flexibility parameters are calculated by imposing that the forces given by FastSim coincide with the forces calculated through an exact theory considering infinite friction coefficient. In this FastSim extension to non-Hertzian areas, the Kalker's steady-state CONTACT method formulated in the preceding subsection is adopted as exact theory.

Under adhesion conditions, any contact model establishes a linear relationship between forces and creepages that can be expressed as

$$\bar{\mathbf{F}} = \mathbf{K}\,\boldsymbol{\xi}\,, \tag{15}$$

where $\bar{\mathbf{F}} = \{\bar{F}_1, \bar{F}_2, \bar{M}_3\}^{\mathrm{T}}$ is the vector with the contact forces and the spin moment when considering adhesion conditions in the entire contact area. The matrix $\mathbf{K}$ contains the creep coefficients, being formulated for Hertzian areas as

$$\mathbf{K}_1 = \begin{bmatrix} -f_{11} & 0 & 0 \\ 0 & -f_{22} & -f_{23} \\ 0 & f_{23} & -f_{33} \end{bmatrix}, \tag{16}$$

so that with $\mathbf{K}_1$, Equation (15) would correspond to Kalker's Linear Theory.

The matrix $\mathbf{K}$ can be derived from the steady-state method with infinite friction coefficient by replacing Equation (11) in (14), and the resulting formulation in (13), hence obtaining

$$\mathbf{F} = S\,\Delta x_1\,\mathbf{D}\,(\mathbf{A} - \mathbf{A}^0)^{-1}\mathbf{D}^{\mathrm{T}}\boldsymbol{\xi}\,, \tag{17}$$

and consequently,

$$\mathbf{K}_2 = S\,\Delta x_1\,\mathbf{D}\,\left(\mathbf{A} - \mathbf{A}^0\right)^{-1}\mathbf{D}^{\mathrm{T}}\,. \tag{18}$$

On the other hand, the nH-FastSim extension permits to deduce the contact force vector $\bar{\mathbf{F}}$ from Equations (4) and (13)

$$\mathbf{F} = S\,\mathbf{D}\,\mathbf{B}\,\mathbf{L}^{-1}\,\boldsymbol{\xi}. \tag{19}$$

From this expression, the matrix $\mathbf{K}$ for the nH-FastSim method can be obtained

$$\mathbf{K}_3 = S\,\mathbf{D}\,\mathbf{B}\,\mathbf{L}^{-1}. \tag{20}$$

As the contact patches are no longer elliptical, terms f_{12}, f_{13}, f_{21} and f_{31} of matrices $\mathbf{K}_2$ and $\mathbf{K}_3$ are non-zero due to the asymmetry of the contact area.

Matching the tangential forces of both methods means forcing matrices $\mathbf{K}_2$ from the full-adhesion exact method and $\mathbf{K}_3$ from nH-FastSim to be equal. From this equality, $\mathbf{L}$ matrix can be obtained as

$$\mathbf{L} = S\,\mathbf{K}_2^{-1}\,\mathbf{D}\,\mathbf{B}\,, \tag{21}$$

from where the flexibility parameters are derived from the entries of $\mathbf{L}$ on the diagonal (Equation (5)). Nevertheless, this procedure, in which the non-zero terms are taken into account, did not give accurate results for the flexibility parameters, contrary to what other researchers found [8, 12, 18]. This loss of accuracy led us to use the methodology proposed by Kalker in his FastSim development [5]: the tangential contact forces given by the full-adhesion steady-state CONTACT model in Equation (17), in which the non-zero terms are neglected, are equated term by term with the forces given by nH-FastSim in Equation (19), providing the flexibility parameters that compute more precise contact forces for non-Hertzian cases.

3. Creepage coefficients through contact

The ability of the nH-FastSim algorithm to obtain acceptable results is conditioned by the precision in the calculation of the creepage coefficients through the steady-state CONTACT method, which will be tested in this section. Kalker's Linear Theory is used in this analysis as reference solution since it is the only known theory that provides exact results under adhesion conditions. This fact limits to conduct this evaluation exclusively for elliptical areas.2

The steady-state CONTACT is based on the collocation method: the solution of the fundamental equation must be fulfilled in a finite number of points in the spatial domain. Consequently, the behaviour of this numerical model depends fundamentally on the position and the number of the collocation points and the shape of the domain. The position refers, in this case, to the relative location of the point within each element of the mesh; the number of points is associated with the mesh refinement, and the shape of the domain is analysed through the ratio between the semiaxes of the contact ellipse. All these studies are carried out for the dimensions of a railway case (normal load of 10 tons, wheel and rail Young's modulus of $E = 2.1 \times 10^{11}$ N/m^2), except the Poisson's ratio, which is varied through the different studies.

3.1. Influence of the collocation point

The x_1-coordinate of the collocation point with respect to the centre of the element is defined by $\alpha\,\Delta x_1/2$, being Δx_1 the longitudinal dimension of the element, and α a dimensionless parameter (see Figure 2).

Figure 3 illustrates the influence of the collocation point location on the relative error for the creepage coefficients calculation through the CONTACT model performed at UPV. This study has been carried out for five different ellipses, defined by their semiaxes ratio $r = a/b$. Figure 3(A and B) show that the lowest relative error values in coefficients C_{11} and C_{22} are achieved when the collocation point is located at the centre of the element. Conversely, the lowest errors in coefficient C_{23} calculation occur for $\alpha = 0.5$ (see Figure 3C).
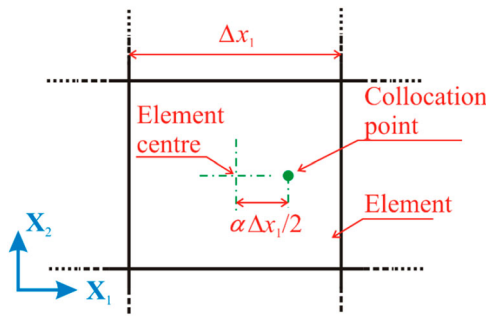
Figure 2. Element of the mesh with a collocation point.
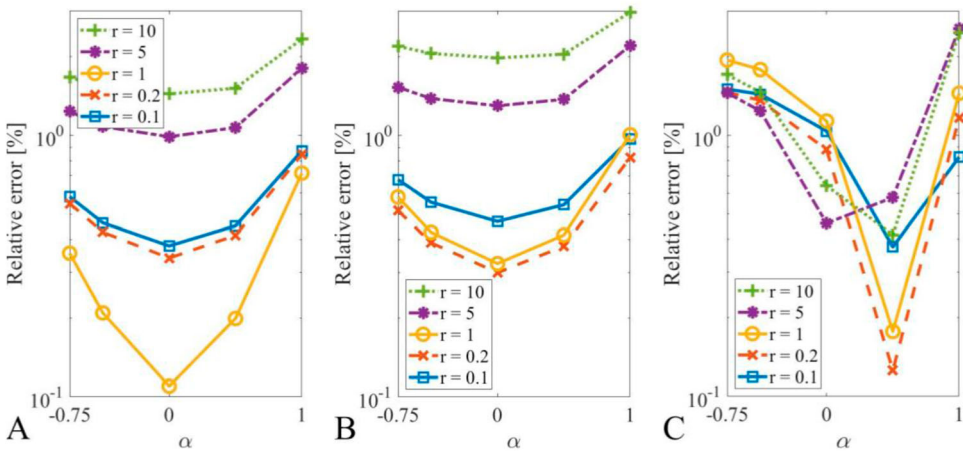

Figure 3. Influence of the collocation point location for an 80 × 80 mesh and five different ellipse geometries on the creepage coefficients: (A) C_{11} coefficient; (B) C_{22} coefficient; (C) C_{23} coefficient.

3.2. Influence of the element size

Figure 4 shows the relative error in the calculation of the creepage coefficients as a function of the mesh refinement. As a refinement control parameter, the total number of elements in contact N_C is used. As in the previous section, the calculation has been carried out for five semiaxes ratios.

The program developed by the authors of CONTACT program with infinite friction coefficient presents an error below 2% for meshes with 2800 elements in contact, although the tendency does not present convergence since errors do not decrease to zero. The full-adhesion hypothesis makes the tangential tractions at the trailing edge of the contact area tend to infinity, producing numerical errors and the non-convergence of the method due to the singularity in the domain [8], but allows obtaining results that provide acceptable precision. Despite this, for meshes with 2800 elements in contact, errors are below 2% in all the studied cases (with an error average of 0.8%) even for the most distorted ellipse ($r = 10$), validating the use of this approach for simulation in railway dynamics.
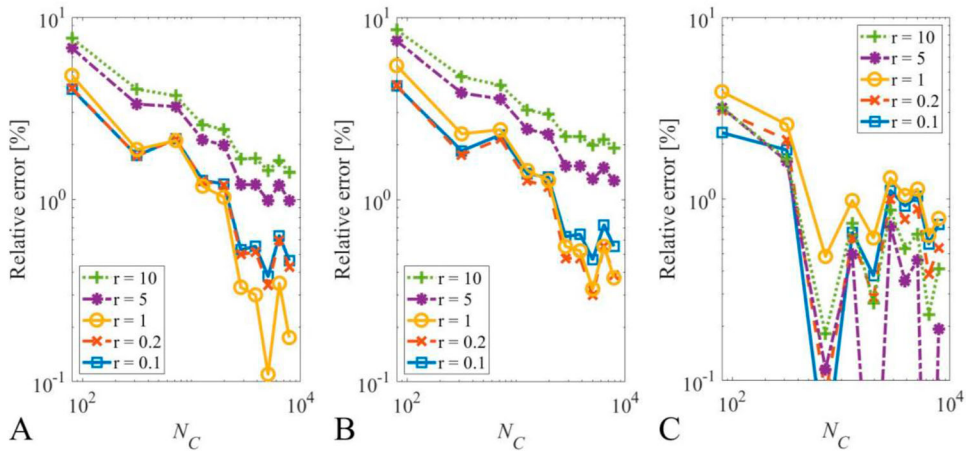
Figure 4. Influence of the element size (through the number of elements in contact N_C) for five different ellipse geometries and $\alpha = 0$ on the creepage coefficients: (A) C_{11} coefficient; (B) C_{22} coefficient; (C) C_{23} coefficient.

3.3. Influence of the contact area shape

Table 1 presents the relative error obtained when calculating the creepage coefficients C_{ij} for the values of semiaxes ratio r and Poisson's ratio υ proposed in the well-known table published in Ref. [13] and other railway monographs and papers. It can be observed an increasing error trend with the ellipse ratio a/b for the coefficients C_{11} and C_{22}, contrary to the proneness shown for C_{23}. Except for the most extreme cases of ellipse ratios, the computed errors through the CONTACT program developed by the authors are below 1%, being slightly higher for C_{23}.

4. Results

This section summarises the results of nH-FastSim, which may contribute to its validation for the computing of the contact problem for realistic cases. Table 2 gathers a test-set compatible with a realistic value for the normal load per axle and a range of creepages plausible under normal circumstances for existing wheel (S1002) and rail profiles (UIC60). The simulations performed give the creep forces and traction distribution for the study case summarised, together with the associated computational cost, which is compared with our implementation of the steady-state CONTACT method. The study also analyses various lateral positions of the wheelset with respect to its position centred on the track.

The normal contact problem is solved through the methodology described in Ref. [19] for the different wheelset positions studied. The location of the wheelset is considered through its lateral displacement y, assuming null yaw angle. For the analysed wheel, a negative displacement $y < 0$ comes closer the contact area to the wheel flange. In Ref. [20], the difference of the rolling radii for different wheelset positions can be found, for the same model data than the one gathered in Table 2.

In this section, normalised values of longitudinal ξ' and lateral η' creepage are considered, which represent the beginning of the full slip condition when $||(\xi', \eta')|| \approx 1$ (it would

Table 1. Relative error (in %) associated with the calculation of the creepage coefficients C_{ij} by means of the steady-state CONTACT model for adhesion conditions.

	C_{11} relative error			C_{22} relative error			C_{23} relative error		
	$v = 0$	$v = 1/4$	$v = 1/2$	$v = 0$	$v = 1/4$	$v = 1/2$	$v = 0$	$v = 1/4$	$v = 1/2$
a/b									
0.1	0.43%	0.53%	0.61%	0.43%	0.63%	0.49%	1.05%	1.11%	1.33%
0.2	0.41%	0.50%	0.53%	0.41%	0.48%	0.55%	1.17%	1.00%	0.98%
0.3	0.51%	0.66%	0.59%	0.51%	0.55%	0.69%	1.26%	1.03%	1.00%
0.4	0.46%	0.53%	0.58%	0.46%	0.51%	0.46%	1.29%	1.15%	0.96%
0.5	0.52%	0.56%	1.17%	0.52%	0.56%	0.70%	1.27%	1.17%	0.67%
0.6	0.62%	0.42%	0.60%	0.62%	0.65%	0.66%	1.16%	0.69%	1.33%
0.7	0.41%	0.61%	0.65%	0.41%	0.42%	0.63%	0.97%	1.02%	1.47%
0.8	0.53%	0.58%	0.45%	0.53%	0.49%	0.60%	0.90%	1.22%	1.26%
0.9	0.62%	0.57%	0.56%	0.62%	0.54%	0.55%	0.88%	1.31%	0.83%
b/a									
1.0	0.41%	0.33%	0.56%	0.41%	0.55%	0.73%	0.89%	1.31%	0.86%
0.9	0.51%	0.61%	0.43%	0.51%	0.65%	0.83%	0.81%	1.08%	1.05%
0.8	0.52%	0.59%	0.44%	0.52%	0.60%	0.78%	0.87%	1.29%	0.75%
0.7	0.75%	0.56%	0.43%	0.75%	0.73%	0.99%	0.88%	1.06%	1.08%
0.6	0.61%	0.49%	0.41%	0.61%	0.84%	1.19%	1.28%	1.16%	0.97%
0.5	0.87%	0.63%	0.44%	0.87%	0.91%	1.20%	1.06%	0.81%	0.62%
0.4	0.81%	0.81%	0.60%	0.81%	1.03%	1.36%	1.11%	0.88%	0.63%
0.3	1.15%	0.86%	0.70%	1.15%	1.30%	1.60%	1.03%	0.88%	0.53%
0.2	1.39%	1.21%	0.97%	1.39%	1.52%	1.82%	0.92%	0.71%	0.53%
0.1	1.90%	1.67%	1.44%	1.90%	2.22%	2.21%	0.47%	0.87%	0.50%

Table 2. Model data.

Rail profile	UIC60
Rail inclination	1/40
Track gauge	1435 mm
Wheel profile	S1002
Wheel diameter	900 mm
Vertical load per wheelset	200 kN
Wheel and rail Young modulus	$2.1\ 10^{11}$ N/m^2
Wheel and rail Poisson ratio	0.3
Friction coefficient	0.4
Nr. of mesh elements	2800

be a normalisation with respect to saturation conditions). The normalised creepage values ξ' and η' were proposed in Ref. [13] for elliptical areas and calculated according to the following formulas:

$$\xi' = \xi \frac{f_{11}}{3\mu F_3}, \tag{22}$$

$$\eta' = \eta \frac{f_{22}}{3\mu F_3}. \tag{23}$$

For the studies carried out in this section, an extension of the previous formulas will be made to the non-Hertzian case by using the creep coefficients f_{11} and f_{22} obtained numerically from the matrix $\mathbf{K}_2$ in Equation (18). In order to adopt realistic creepage spin values, these are calculated as the projection of the angular velocity of the wheelset to the normal direction to the contact area, normalised with respect to the vehicle speed. Therefore, the

spin is estimated through the following formula

$$\phi = \frac{2}{d} \sin \gamma, \tag{24}$$

where d is the diameter of the wheel and γ its conicity at the contact point. In this way, ϕ becomes dependent of the lateral displacement y through the wheel conicity γ.

4.1. Tangential forces calculation

Figure 5 shows the relative error associated with the calculation of the total tangential force through nH-FastSim, which is computed as follows

$$\text{Relative error} = \frac{|F - F^C|}{F^C}, \tag{25}$$

F being the total tangential force modulus obtained by means of nH-FastSim, and F^C the one calculated through the steady-state CONTACT program developed by the authors. This result is computed as a function of the lateral displacement y for various values of normalised creepages ξ' and η'. When a non-zero spin creepage value is considered, it is calculated according to Equation (24) depending on the lateral displacement y. Since only single contact areas are analysed in this work, the wheelset lateral displacement is varied between ± 4.5 mm (multiple contact areas appear for greater absolute values [19]). In general, the results present an error less than 4% in the estimation of the total tangential force, showing the highest values when the wheelset is centred on the track (case of less elliptical contact area).

Errors obtained with the proposed method are below 5% in all study cases, which is in accordance with FastSim error results presented by other authors [21], since neither pure spin cases nor realistic cases with combined longitudinal, lateral and spin creepage are analysed in the present work (only realistic cases were pretended to be analysed).

4.2. Tangential traction distribution

Figure 6 shows the tangential traction distribution calculated for the contact area corresponding to the wheelset centred on the track (as just indicated, the position for which the model produces worse force results due to the resulting non-elliptical contact patch). The analysis is performed for different load conditions with different creepages imposed. These creepage combinations have been chosen in order to analyse the influence of the creepage direction on the tangential traction distribution: only longitudinal creepage (Figure 6A and D), lateral and spin creepages (Figure 6B and E) and combined longitudinal, lateral and spin creepages (Figure 6C and F). The calculations have been carried out by means of both nH-FastSim and the steady-state CONTACT (authors' own implementation), showing that the first one underestimates the slip area, especially when creepages are combined.

Figure 7 gathers the creep curves for the longitudinal contact force under different wheelset lateral displacements and lateral creepage values, with the aim of studying the influence of the contact area shape and the combination of creepages. Results in this figure show an accurate approximation of the proposed nH-FastSim extension when comparing with the exact solution provided by the steady-state CONTACT program used, with similar
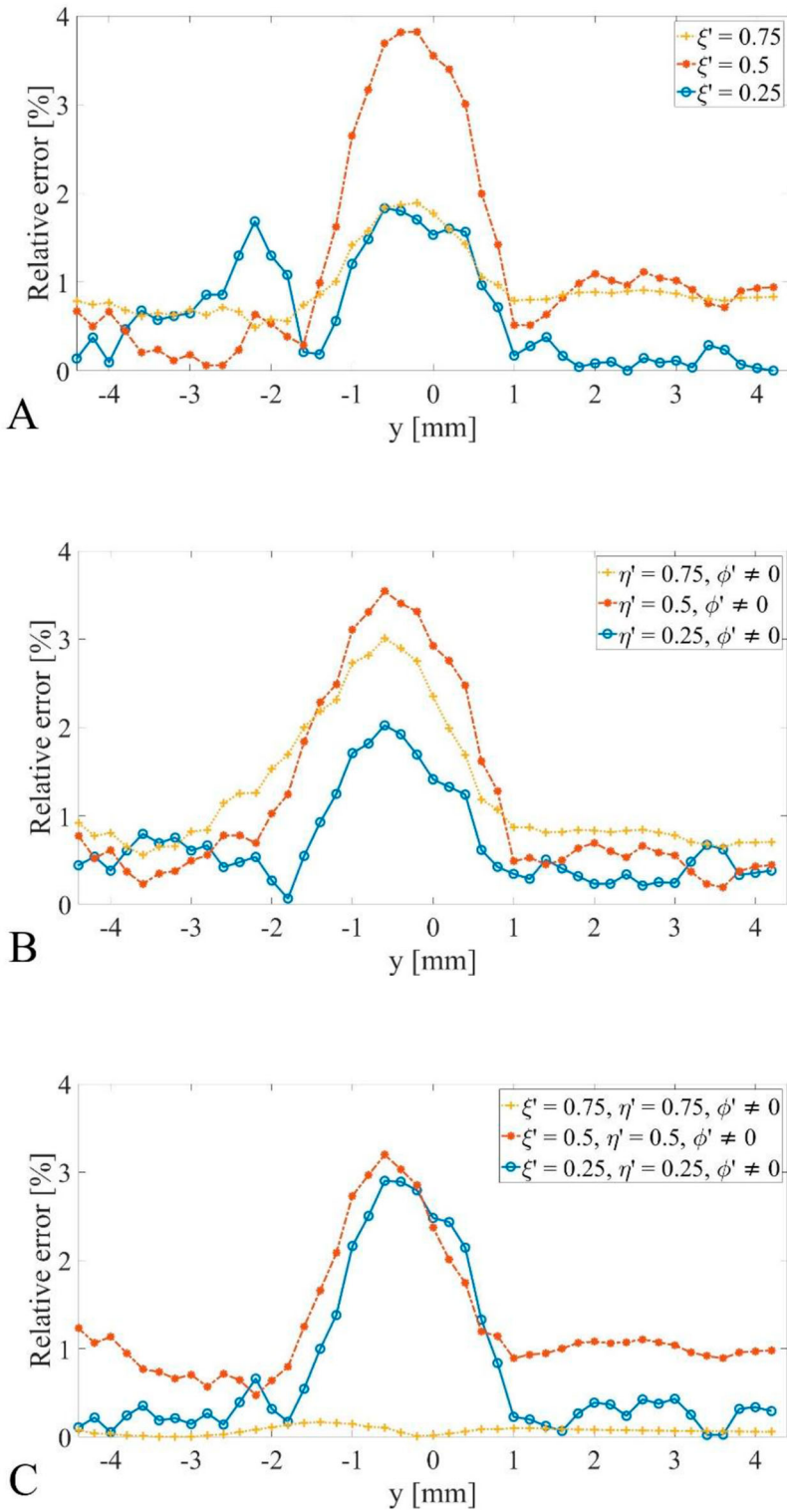
Figure 5. Relative error in the tangential total force as a function of the wheelset lateral displacement y for: (A) pure longitudinal creepage ($\eta' = \phi' = 0$); (B) lateral creepage with spin ($\xi' = 0$); (C) general case.
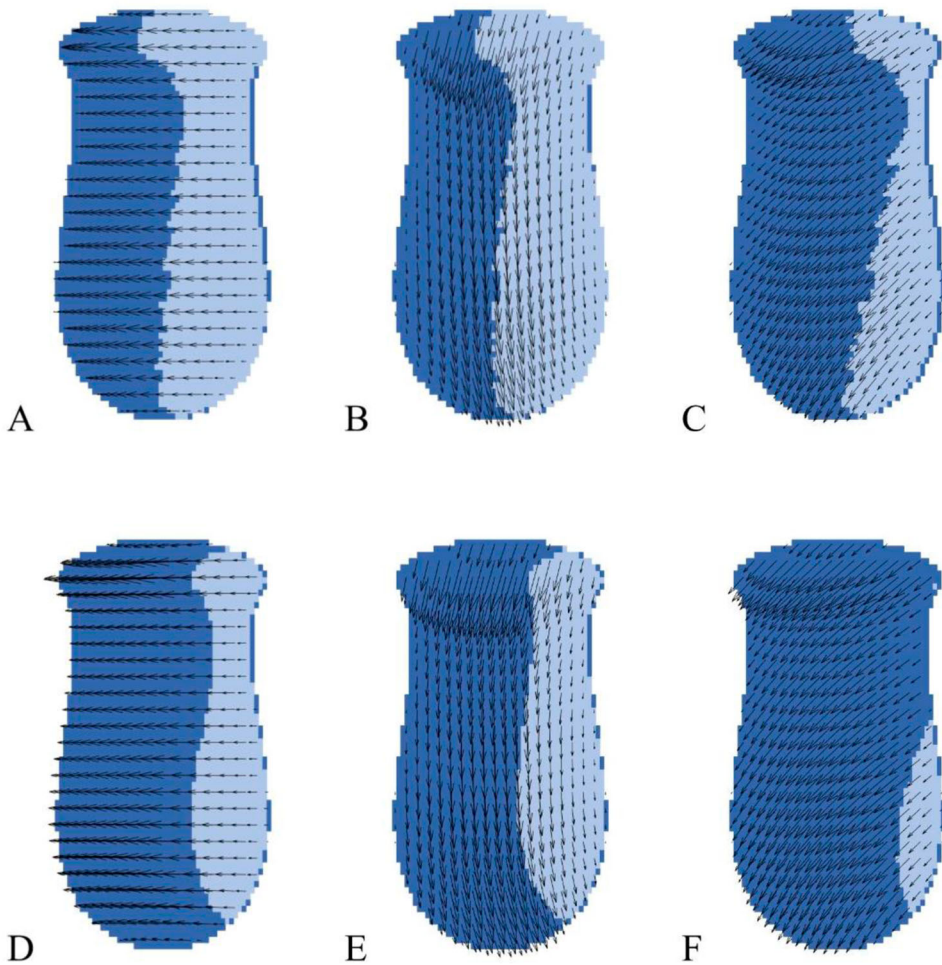
Figure 6. Tangential traction distribution for a wheelset lateral displacement $y = 0$ mm. Upper row corresponds to nH-FastSim, and lower row to the steady-state CON-TACT results. Darker colour background indicates slip area. Results have been obtained for different creepages: (A) and (D) $\xi' = 0.5$; (B) and (E) $\eta' = 0.5, \phi' \neq 0$; (C) and (F) $\xi' = 0.5, \eta' = 0.5, \phi' \neq 0$.

errors in the results shown in Figure 5 (lower than 4%). The initial linear region, equivalent to consider infinity friction coefficient, perfectly overlaps and the saturation values end up coinciding for the simulated cases. Larger errors are found when the wheelset is centred on the track (again in line with Figure 5) and when combined creepages are imposed (according to Figure 6).

4.3. Computational time

Figure 8 compares the algorithm speed with respect to the steady-state CONTACT version used by the authors. To this aim, computational times required by steady-state CONTACT
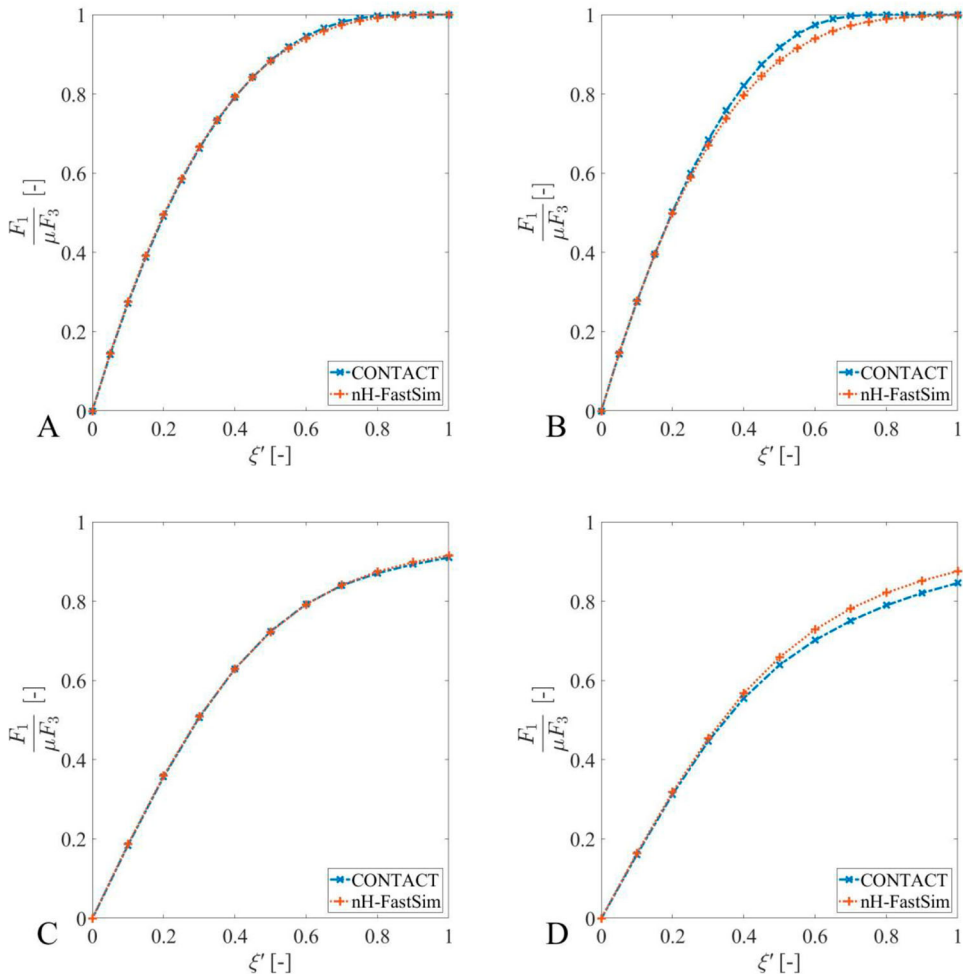
Figure 7. Longitudinal force as a function of the longitudinal creepage for different studies: (A) $y = -0.003$ m, $\eta' = 0$; (B) $y = 0$ m, $\eta' = 0$; (C) $y = -0.003$ m, $\eta' = 0.5$; (D) $y = 0$ m, $\eta' = 0.5$.

and nH-FastSim are collected for simulations run in Matlab© through a PC with the following specifications: Intel(R) Core (TM) i7-9700 CPU 3.0 GHz with 64.00 GB of RAM and 64-bit computing. For the same study case, Figure 8A plots the absolute computational time required by both methods for a sweep in the number of elements in contact N_C; the creepage values and the lateral displacement are randomly selected according to a uniform distribution. Figure 8B shows the computational performance through the ratio between the calculation times computed for both methods for the same study cases. In general, the times associated with nH-FastSim are one order below the steady-state CONTACT programmed by the authors, performance that will be different from other implementations and enhancements (such as those proposed in Ref. [22]). The trend of the increase in computational cost with the number of elements is approximately linear when it is plotted on a logarithmic scale.
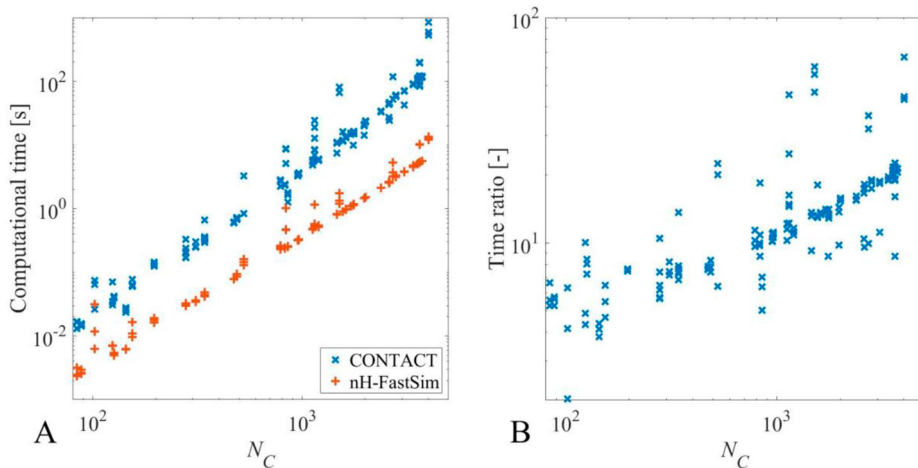
Figure 8. Computational times vs. number of mesh elements in contact N_C for random values of creepages and wheelset lateral displacements: (A) absolute computational times for both CONTACT and nH-FastSim methods; (B) time ratio.

5. Conclusions

In this work, a methodology based on the FastSim algorithm is presented to solve the tangential problem with improved computational features in the case that the Hertzian contact conditions are not met. The formulation presents a parallelism with the original method, differing in the type of discretisation (a regular mesh is adopted in the proposed one) and in the calculation of the flexibility parameters, since Kalker's Linear Theory is only applicable for elliptical areas. To get around this issue, an alternative simplified method named nH-FastSim is implemented so as to obtain the forces under adhesion conditions for non-elliptical areas. It leads to the need of adapting the steady-state CONTACT program for adhesion areas, which allows to compute the creepage coefficients with errors lower than 2% when selecting the collocation point at the centre of the mesh element. When compared with the steady-state CONTACT that implements the Coulomb's law regularisation, nH-FastSim produces acceptable levels of precision, significantly reducing the maximum error below 4% for the creep forces in the non-Hertzian contact simulations performed, while the computational times required are between 10 and 20 times lower than the steady-state CONTACT with the Coulomb's law regularisation. Consequently, the proposed extension of FastSim can be shown as a tool compatible with other improvements implemented in CONTACT that lead to the reduction of its computational cost, such as those included in Ref. [22].

Disclosure statement

Funding

ORCID

L. Baeza ⓘ http://orcid.org/0000-0002-3815-8706

References

[1] Kalker JJ. Book of tables for the Hertzian creep-force law. Presented at the Proc. 2nd Mini Conf. Contact Mech. Wear Rail/Wheel Syst., Budapest, 1996.

[2] Vermeuien PJ, Johnson KL. Contact of nonspherical elastic bodies transmitting tangential forces. J Applied Mechanics, Transactions ASME. 1964;31(2):338–340. doi:10.1115/1.3629610.

[3] Shen ZY, Hedrick JK, Elkins JA. Comparison of alternative creep force models for rail vehicle dynamic analysis. In Dynamics of Vehicles on Roads and on Tracks, Proceedings of IAVSD Symposium, 1984, pp. 591-605.

[4] Polach O. Fast wheel-rail forces calculation computer code. Veh Syst Dyn. 2000;33(SUPPL.): 728–739. doi:10.1080/00423114.1999.12063125.

[5] Kalker JJ. A fast algorithm for the simplified theory of rolling contact. Veh Syst Dyn. 1982;11(1):1–13. doi:10.1080/00423118208968684.

[6] Kalker JJ. On the rolling contact of two e lastic bodies in the presence of dry friction [PhD]. T.U. Delft, 1967.

[7] Piotrowski J, Kik W. A simplified model of wheel/rail contact mechanics for non-Hertzian problems and its application in rail vehicle dynamic simulations. Veh Syst Dyn. 2008;46(1-2):27–48. doi:10.1080/00423110701586444.

[8] Alonso A, Giménez JG. Tangential problem solution for non-elliptical contact areas with the FastSim algorithm. Veh Syst Dyn. 2007;45(4):341–357. doi:10.1080/00423110600999763.

[9] Piotrowski J, Liu B, Bruni S. The Kalker book of tables for non-Hertzian contact of wheel and rail. Veh Syst Dyn. 2017;55(6):875–901. doi:10.1080/00423114.2017.1291980.

[10] Linder C. Verschleiss von Eisenbahnrädern mit Unrundheiten [PhD]. ETH Zürich, 1997.

[11] Ayasse JB, Chollet H. Determination of the wheel rail contact patch in semi-hertzian conditions. Veh Syst Dyn. 2005;43(3):161–172. doi:10.1080/00423110412331327193.

[12] Knothe K, Hung LT. A method for the analysis of the tangential stresses and the wear distribution between two elastic bodies of revolution in rolling contact. Int J Solids Struct. 1985;21(8):889–906. doi:10.1016/0020-7683(85)90040-X.

[13] Kalker JJ. Three-dimensional elastic bodies in rolling contact. Dordrecht: Kluwer Academic Publishers; 2018.

[14] Sichani MS, Enblom R, Berg M. Comparison of non-elliptic contact models: towards fast and accurate modelling of wheel-rail contact. Wear. 2014;314(1-2):111–117. doi:10.1016/j.wear.2013.11.047.

[15] Ma X, Wang P, Xu J, et al. Comparison of non-Hertzian modeling approaches for wheel–rail rolling contact mechanics in the switch panel of a railway turnout. Proceedings of the Institution of Mechanical Engineers, Part F: Journal of Rail and Rapid Transit. 2019;233(4):466–476. doi:10.1177/0954409718799825.

[16] Kalker JJ. Two algorithms for the contact problem in elastostatics. Article no. (eds.), Waterloo, Canada, Waterloo Univ. Press, 1983, Part 2, p.103-120., 1983.

[17] Vollebregt EAH, Wilders P. FASTSIM2: a second-order accurate frictional rolling contact algorithm. Comput Mech. 2011;47(1):105–116. doi:10.1007/s00466-010-0536-7.

[18] Alonso A, Giménez JG, Martín LM. Spin moment calculation and its importance in railway dynamics. Proceedings of the Institution of Mechanical Engineers, Part F: Journal of Rail and Rapid Transit. 2009;223(5):453–460. doi:10.1243/09544097JRRT262.

[19] Baeza L, Thompson DJ, Squicciarini G, et al. Method for obtaining the wheel–rail contact location and its application to the normal problem calculation through 'CONTACT'. Veh Syst Dyn. 2018;56(11):1734–1746. doi:10.1080/00423114.2018.1439178.

[20] Yang G. Dynamic analysis of railway wheelsets and complete vehicle systems [PhD]. T.U. Delft, 1993.

[21] Vollebregt EAH, Iwnicki SD, Xie G, et al. Assessing the accuracy of different simplified frictional rolling contact algorithms. Veh Syst Dyn. 2012;50(1):1–17. doi:10.1080/00423114.2011.552618.

[22] Vollebregt EAH. A new solver for the elastic normal contact problem using conjugate gradients, deflation, and an FFT-based preconditioner. J Comput Phys. 2014;257:333–351. doi:10.1016/j.jcp.2013.10.005.

[23] Giner J, Baeza L, Vila P, et al. Study of the falling friction effect on rolling contact parameters. Tribol Lett. 2017;65(1). doi:10.1007/s11249-016-0810-8.

[24] Baeza L, Vila P, Roda A, et al. Prediction of corrugation in rails using a non-stationary wheel-rail contact model. Wear. 2008;265(9-10):1156–1162. doi:10.1016/j.wear.2008.01.024.

Appendix

The solution of Equation (10) is originally carried out through Kalker's TANG algorithm and Newton iteration (an iterative process in which systems of equations are solved from successive hypotheses about if the elements belong to the adhesion or the slip area, see Ref [13]). The calculation procedure can be accelerated if the regularisation of the Coulomb's law is implemented [23]. According to this approach, the tangential tractions in the e-th element of the mesh are approximated through the formula

$$p_\tau^e = \frac{-2\mu\,p_3^e}{\pi}\mathrm{atan}\left(\frac{||(s_1^e, s_2^e)||}{\varepsilon}\right)\frac{s_\tau^e}{||(s_1^e, s_2^e)||}, \quad \tau = 1, 2, \tag{A1}$$

being ε sufficiently small ($\varepsilon = 10^{-8}$m/s is chosen in this paper). Figure A1 shows the behaviour of the tangential traction with the slip velocity for different ε.

This procedure allows formulating Equation (10), being the slip velocity vector **s** as the only unknown variable after introducing Equation (A1) in (10) [24]. The resulting equation is solved by means of a Newton-Raphson scheme, in which **s** is the unknown variable. Once the slip velocity vector is obtained, tangential tractions distribution can be obtained through Equation (A1). This method leads to the steady-state CONTACT solution used as reference for the later validation of the proposed FastSim extension.
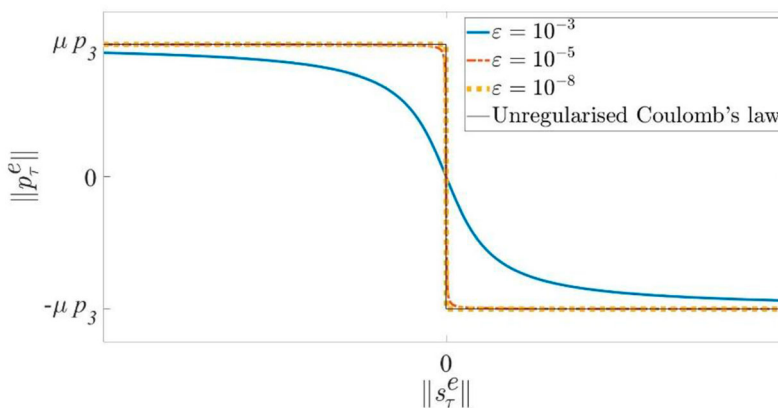

Figure A1. Coulomb's law regularisation for different values of ε parameter.